

1 Article

2 Effect of Bi₂O₃ doping on the mechanical properties 3 of PbO ceramic pellets used in lead-cooled fast 4 reactors

5 Yan Ma ^{1,*}, Anxia Yang ¹, Huiping Zhu ¹, Arslan Muhammad ¹, Pengwei Yang¹, Bokun Huang ¹
6 and Fenglei Niu ¹

7 ¹ Key Laboratory of Passive Nuclear Power Safety and Technology, North China Electric Power University,
8 Beijing 102206, P.R. China; mayan@ncepu.edu.cn

9 * Correspondence: mayan@ncepu.edu.cn

10

11 **Abstract:** In this paper, the effect of Bi₂O₃ doping on the mechanical properties of PbO ceramic
12 pellets was studied. For this purpose, different ratios of Bi₂O₃/PbO (i.e., xBi₂O₃–(1-x)PbO, where x
13 is 0, 1, 3, 5, 7 wt%) were fabricated and sintered at 570, 620, and 670°C. Mechanical properties
14 including density, hardness, flexural strength, and sintering of PbO were studied for the
15 aforementioned compositions. Phase compositions, microstructures, and worn surfaces of the
16 composites were characterized by scanning electron microscopy and X-ray diffraction (XRD). The
17 XRD analysis revealed that a solid solution formed in the composite ceramic. The best suited
18 conditions of temperature and doping of Bi₂O₃ for optimal sintering are 620°C and 3 wt%,
19 respectively. The hardness of the 3 wt% Bi₂O₃–97 wt% PbO ceramic was 717 MPa, which is
20 about four times higher than the hardness of pure PbO; in addition, the strength of the composites
21 was 43 MPa, which is two times higher than that of pure PbO. The integrity of the composites was
22 verified using the lead–bismuth eutectic alloy flushing experiment. Results of this research paper
23 are important for future studies of oxygen control in the lead–bismuth eutectic alloy of lead-cooled
24 fast reactors.

25 **Keywords:** Bi₂O₃; PbO; sintering temperature; mechanical properties; lead–bismuth eutectic alloy.
26

27 1. Introduction

28 Lead oxide (PbO) ceramic pellets are used in solid-phase oxygen control systems, which are
29 an important constituent of lead-cooled fast reactors (LFRs). In LFRs, the lead–bismuth eutectic (LBE)
30 alloy was chosen as a coolant material [1]. However, LBE can cause severe corrosion of structural
31 materials [2], including pipes and other components. To prevent such corrosion, it is important to
32 consider appropriate protective methods. Studies in the past have shown that oxygen is the most
33 critical element in the corrosion caused by LBE alloys. When oxide layers of a certain thickness get
34 coated on the internal surface of the steel pipes, forming a film of magnetite ferroferric oxide and iron
35 chrome spinel- $[Fe_{(3-x)}Cr_x]O_4$, it prevents the further penetration of LBEs. The thickness of the oxide
36 layer varies at different levels of oxygen concentration; an oxide layer that is too thick or too thin
37 cannot protect the steel well [3]. Many research studies have shown that solid-phase oxygen control
38 is a promising anti-corrosion method [4]. In this approach, the PbO ceramic pellets are set inside and
39 liquid metal and oxygen ions are released from the ceramic pellets into the liquid metal. The
40 concentration of oxygen ions in the liquid metal can be adjusted by the low rate and temperature of
41 the coolant. To keep the coolant pure and to protect the steel pipe, high-strength PbO ceramic pellets
42 are required, which have fast oxygen concentration regulation and crack resistance during operation.

43 Currently, experiments on solid-phase control systems are being carried out in the LBE test
44 loop CRAFT at SCK•CEN in Mol, Belgium [5], in the Pb–Bi forced convection loop in Ibaraki, Japan
45 [6], and as part of the DEMETRA project by CEA, Saclay in Gif-sur-Yvette, France [7]. Though
46 several studies have been done theoretically and practically on solid-phase control systems, only a
47 few have reported on the mechanical properties and microstructures of PbO. Hence, research on
48 developing sintering techniques of PbO ceramic pellets that will have excellent performance during
49 operation has become a hot topic in this area.

50 Some studies have reported that the PbO ceramic pellets tested in CRAFT loop were cracked in
51 the area of equator during the experiment (Fig. 1). PbO ceramic pellets broken in the loop can result
52 in debris being formed in the coolant, eventually blocking the pipeline in extreme cases [5]. Kondo et
53 al. found that PbO powder was sintered in the form of lumps at 800°C, following which the lumps
54 were mechanically broken into small pieces [6]. The relative density of the PbO ceramic pellets in the
55 above loop was 72.82%. Brissonneau reported that the PbO pellets were generated from PbO powder
56 and water under a force of 45 kN at the pellet for 2 min, and then the pellets were sintered at 620°C
57 for 2h at a slow temperature ramp ($2^{\circ}\text{C}\cdot\text{min}^{-1}$) [7]. The ceramic pellets discussed above are used as
58 PbO pellets in oxygen concentration control experiments, but there is no detailed literature on the
59 properties of PbO ceramic pellets. It can be seen from Fig. 1 that the PbO ceramic pellets used in the
60 experiment were not high in strength and could be easily cracked along the equatorial plane because
61 of their spherical shape.

62 We have enhanced our scope of research to improve the mechanical properties and avoid the
63 cracking of PbO ceramic pellets in the LBE alloy. Doping by Pb powder using liquid-phase sintering
64 improved the mechanical properties of the ceramic pellets [8]. The mechanical properties and
65 microstructures of the Pb, PbO, and Pb_3O_4 ceramic pellets were also studied in detail, and the results
66 showed that the addition of lead powder facilitates sintering and increases the strength of the
67 ceramic. We also used the microwave sintering technique to improve the strength of the PbO ceramic
68 pellets [9]. However, there was no significant improvement in the mechanical properties and the
69 technique resulted in the occurrence of cracks.

70 In this study, Bi_2O_3 powder as the sintering aid was added to the PbO precursor. Bi_2O_3 powder
71 was chosen as the sintering agent for two reasons: (1) the raw material of the ceramic pellets will not
72 cause pollute the coolant or make it impure and (2) the diameter of Bi^{3+} is similar to the diameter of
73 Pb^{2+} and their chemical properties are very similar, which is beneficial in the sintering process. In this
74 paper, the mechanical properties and microstructures of $\text{Bi}_2\text{O}_3/\text{PbO}$ with different compositions (i.e.,
75 $x\text{Bi}_2\text{O}_3-(1-x)\text{PbO}$, where x is 0, 1, 3, 5, 7 wt%) were investigated in terms of their strength, hardness,
76 and scanning electron microscopy (SEM) data to arrive at the optimal value of x and the sintering
77 temperature. Flushing experiments were then performed to verify the integrity of PbO ceramic
78 pellets.
79



80
81
82 Figure 1. PbO ceramic pellets tested in the CRAFT loop and MEXICO loop [5].
83

84 2. Materials and Methods

85 The chemical composition of the ceramic was chosen to be $x\text{Bi}_2\text{O}_3-(1-x)\text{PbO}$ (the value of x is 0,
86 1, 3, 5, 7 wt%) for conventional sintering. The initial Bi_2O_3 and PbO powders (A.R. 99% purity) were
87 purchased from Sinopharm Chemical Reagent Co. Ltd., Beijing, China. The powders were mixed and
88 ground using a planetary ball mill with 2 wt% deionized water for 24 h. The green compact was
89 fabricated using a cold steel die at a uniaxial pressure of 40 MPa. The rate of pressure during
90 compression and depression was kept controlled below 0.5 MPa/s, in order to reduce the elastic
91 aftereffect and avoid the splitting of the compact. The specimens were then sintered at 570°C, 620°C,
92 and 670°C for 2h at a heating rate of $10^\circ\text{C}\cdot\text{min}^{-1}$, and cooled to room temperature [8].

93 During sintering, the compacts were covered by the PbO powder to further minimize PbO
94 volatilization [10]. It was noticed that the loss of PbO leads to a decrease in density and affects the
95 mechanical properties of PbO ceramic pellets [11]. Disc samples (diameter, 13 mm) and bar samples
96 (4 mm × 3 mm × 35 mm) were fabricated for mechanical property testing. The tablet-like pellets of PbO
97 ceramic pellets (diameter, 6 mm; height, 5 mm) were fabricated to test their integrity using the
98 flushing experiment.

99 Microstructures were observed using a Quanta 200F field emission scanning electron
100 microscope. The crystalline phases were analyzed using a D8 Focus X-ray diffraction with $\text{Cu K}\alpha$
101 radiation. Hardness was estimated on polished samples by the indentation method using a Micro
102 Vickers Hardness Tester. The indentation test was conducted with a load of 0.98 N held for 15 s. The
103 hardness (H_v) was calculated according to ASTM C1327-15 [12] as below:

$$104 \quad H_v = \frac{1.8544F}{d^2}, \quad (1)$$

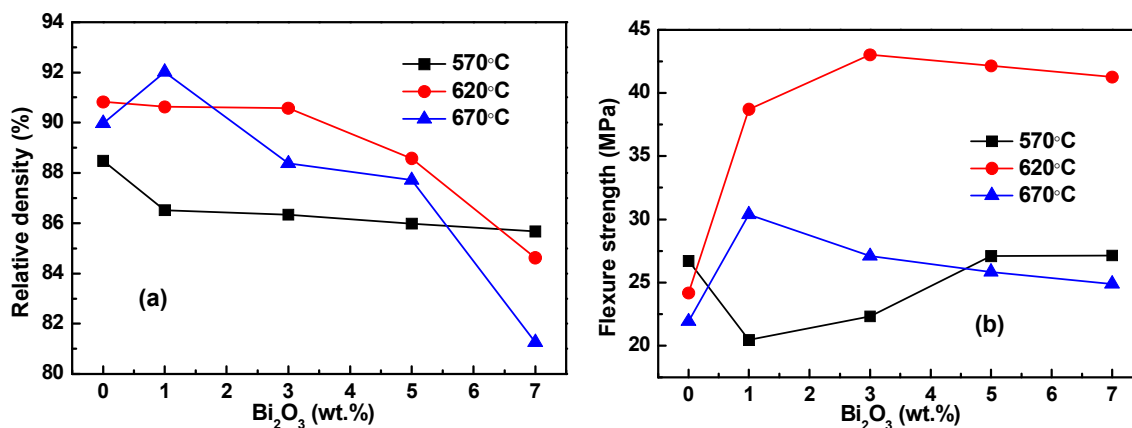
105 where F is the applied load and d is the mean value of the diagonal length of the indentation. A
106 flexural strength test was conducted by the three-point flexural method (span, 35 mm; crosshead
107 speed, $0.5 \text{ mm}\cdot\text{min}^{-1}$) using a WDW-100E computer control electronic universal testing machine. The
108 densities of the specimens were estimated using the Archimedes method by weighing them in air
109 and water. Data were collected for 6–8 samples to obtain an average of results.

110 3. Results

111 3.1 Mechanical properties of Bi_2O_3 - PbO ceramic pellets

112 Figure 2(a) shows the relative densities versus sintering temperatures for PbO ceramic pellets as
113 a function of Bi_2O_3 wt%. The effect of sintering temperature on the density did not show a specific
114 increasing or decreasing trend. The peak value of 92.01% is achieved at 670°C with 1 wt% Bi_2O_3 .
115 Excluding the effects of errors, the best density is achieved at a sintering temperature of 620°C as a
116 whole. From Fig. 2(a), we observe that with the increase in the sintering temperature and the Bi_2O_3
117 content, the sintering process is prolonged, creating more pores and reducing the relative density of
118 the ceramic pellets.

119



120

121 Figure 2. (a) Relative density and (b) flexure strength versus sintering temperature for PbO
 122 ceramics with different Bi₂O₃ wt.%.

123

124 At every sintering temperature, the relative density of the ceramic pellets decreases with the
 125 increase in the Bi₂O₃ content. At a sintering temperature of 620°C and an optimum doping value of 3
 126 wt% Bi₂O₃, a high relative density of 90.57% is achieved. Kondo and Takahashi [6] found that the
 127 relative density is 72.82% for pure PbO ceramic pellets sintered at 800°C, which is lower than that
 128 found in this study. The results indicate that doping by a small amount of Bi₂O₃ significantly
 129 improved the density of PbO ceramic pellets.

130 Figure 2(b) shows the graph of flexural strength with content of Bi₂O₃ wt% at different sintering
 131 temperatures for PbO ceramic pellets. The effect of sintering temperature on the flexural strength is
 132 very prominent and changes significantly with changing temperature. The flexural strength of the
 133 PbO ceramic pellets sintered at 620°C is much higher than that of the samples sintered at 570°C and
 134 670°C.

135 It is well known that pure PbO ceramic pellets are not tough enough to flush in LBE [5]. After
 136 doping with 1 wt% Bi₂O₃ at 620°C, the flexural strength of the PbO ceramic pellets increased by 75%.
 137 It reached the peak value of 43 MPa at 3 wt% Bi₂O₃ and then tended to decrease slightly with further
 138 increase in the Bi₂O₃ content. At 570°C, the strength of the ceramic pellets decreased abruptly when
 139 the Bi₂O₃ increased to 1 wt%, but as the Bi₂O₃ content continued to increase, the strength also
 140 increased and attained a constant value of flexural strength. However, the strength at 670°C was just
 141 the opposite. It increased linearly at 1 wt% Bi₂O₃ and then started to decrease and continued to
 142 decrease. The relationship between strength and porosity is defined by the Griffith equation [13] as
 143 shown below:

$$144 \quad \sigma_f = \frac{(1 - \frac{P}{P_0})^n}{Y\sqrt{c}} \quad , \quad (2)$$

145

$$146 \quad c = c_0 \left[1 - \frac{(P_0 - P)}{3(1 - P)} \right] \quad , \quad (3)$$

147

148 where P_0 and n are constants, P is the porosity, Y is the shape factor, and c_0 is the initial crack
 149 length. Thus, it may be concluded that the strength of the sample is inversely proportional to its
 150 porosity and directly proportional to its density. The strength of the material is also inversely
 151 proportional to its grain size according to the Hall–Petch equation [14] as shown below:

$$152 \quad \sigma_f = \sigma_0 + kd^{-\frac{1}{2}} \quad , \quad (4)$$

153 where k is a constant, σ_0 is the strength of the infinite single crystal, and d is the grain size. The
 154 porosity becomes a dominant factor in decreasing the strength when the Bi₂O₃ content is increased
 155 from 3 to 7 wt% at 620°C or at a higher sintering temperature of 670°C, which was consistent with
 156 the results shown in Fig. 2(a).

157

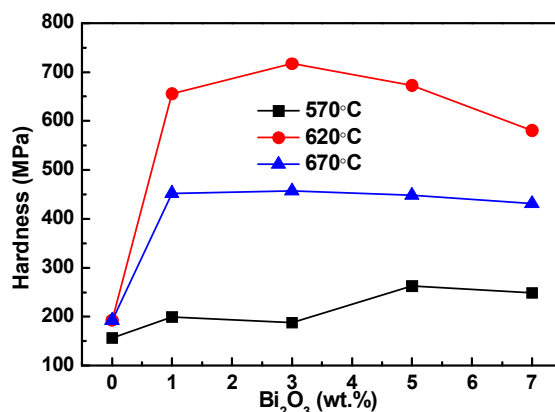


Figure 3. Hardness versus sintering temperature of PbO ceramic pellets with different wt% of Bi₂O₃.

The hardness of the PbO ceramic pellets at different wt% of Bi₂O₃ as a function of temperature is plotted in Fig. 3. It is obvious that the hardness of Bi₂O₃-PbO sintered at 620°C is higher than that at temperatures 570°C and 670°C. At 620°C, the change in hardness is very steep, which increases gradually until the content of Bi₂O₃ is 3 wt%. After reaching its peak, the hardness starts to decline. The optimum hardness of 717 MPa was achieved with 3 wt% Bi₂O₃ at temperature 620°C, which is about four times higher than that of pure PbO.

3.2 Flushing test

Suitable fabricated samples were obtained with a composition of 3 wt% Bi₂O₃-97 wt% PbO, sintered at 620°C. They were then tested in an experimental apparatus for a solid-phase oxygen control system at Beijing Key Laboratory of Passive Safety Technology for Nuclear Energy of North China Electric Power University (Fig. 4).



Figure 4. The experiment bench of the oxygen control system.

In the flushing experiment, 135 ceramic samples of 3 wt% Bi₂O₃-97 wt% PbO were placed in the middle of the mass exchanger. LBE flowed through the PbO ceramic pellets at a speed of 110 L/h for 100 h. The flushing test was carried out at 450°C and the oxygen concentration is 3.14×10^{-4} wt%.

Figure 5 shows the images of the PbO pellets before and after testing. None of the ceramic pellets cracked, which indicated that the strength of the 3 wt% Bi₂O₃-97 wt% PbO ceramic pellets sintered at 620°C is promising to meet the needs of engineering strength requirements.



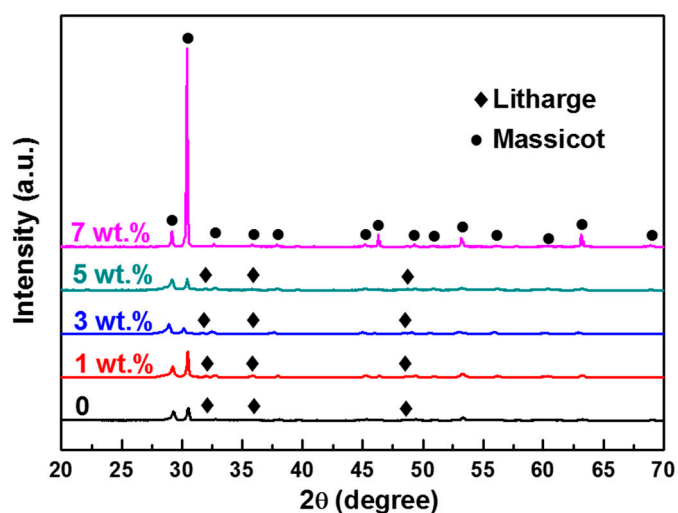
184
185

Figure 5. The 3 wt% Bi₂O₃-97 wt% PbO pellets before and after the flushing experiment.

186 4. Discussion

187 To understand the toughness mechanisms of doping Bi₂O₃, XRD was used to get the patterns of
188 the PbO ceramic pellets sintered at 620°C with different wt% of Bi₂O₃ (Fig. 6). The formation of
189 massicot (PbO, PDF No. 72-0094) was identified as the main crystalline phase, with a small amount
190 of litharge (PbO, PDF No.85-0711). The litharge phase disappeared when the doping was done with
191 more than 5 wt% Bi₂O₃ and the intensity of massicot peaks became stronger. The crystals in the
192 massicot phase were orthogonal ($a=5.489$, $b=4.775$, $c=5.891$) and those in the litharge phase were
193 tetragonal ($a=3.973$, $b=3.973$, $c=5.022$). They are two forms of PbO in nature, and the phase transition
194 temperature is 500°C. The addition of aid promotes the phase transition process, so at high aid
195 content, the main component is massicot. Lead bismuth oxide and Bi₂O₃ phases were not detected in
196 the XRD patterns for the fabricated samples.

197 Figure 6 indicates that the peaks of the PbO phase are shifted to a large angle, which is attributed
198 to the formation of a solid solution between Bi₂O₃ and PbO. The radius of Bi³⁺ (1.03 Å) is smaller than
199 that of Pb²⁺ (1.19 Å). When Bi³⁺ ions are substituted with Pb²⁺ ions, there is a lattice distortion and the
200 resistance to dislocation increases. Therefore, the enhancement of mechanical properties is due to the
201 strengthening of the solid solution of Bi³⁺ ions.



202
203

Figure 6. XRD patterns of PbO ceramic pellets sintered at 620°C with different wt% of Bi₂O₃.

204

205 Figure 7 (a)–(j) shows the SEM micrographs and fracture images of PbO ceramic pellets sintered
206 at 620°C with different wt% of Bi₂O₃. First, with the addition of Bi₂O₃, the grain size of PbO ceramic
207 pellets increases as compared with the pure PbO ceramic pellets. The grain boundaries cannot be
208 seen clearly, which indicates that the sample is at the initial stage of sintering and metallurgical
209 binding has not yet occurred between the powders.

210 When doping is done with 1 wt% Bi₂O₃, the crystals are observed to start growing (Fig. 7(d),
211 indicated by frame). When the Bi₂O₃ content increases to 3 wt%, grains are seen to aggregate to form
212 with distinct grain boundaries (Fig. 7(e)). When the Bi₂O₃ content continues to increase, the solid
213 solution is formed, wherein the solute ions Bi³⁺ replace the host ions Pb²⁺, resulting in the formation
214 of positive ion vacancies, which is beneficial to the sintering process and metallurgical binding
215 [15,16].

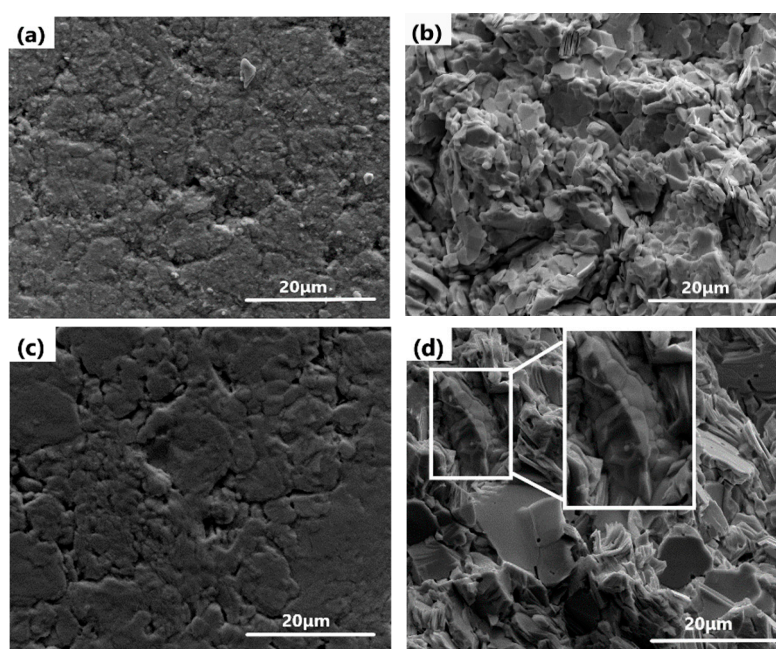
216 Based on the results shown in Fig. 2, xBi₂O₃-(1-x) PbO (x being 0–3 wt%) can be considered to
217 have the same relative density of ~90.6%. Thus, doping of Bi₂O₃ intensifies the sintering process by
218 grain growth at 620°C as the amount of Bi₂O₃ is increased from 0 to 3 wt%. There is almost no change
219 in the size of the grains for 3–7 wt% Bi₂O₃ ceramic pellets as observed by SEM (Fig. 7(e)–(j)). According
220 to Eqs. (2) and (3), it is seen that the effect of porosity on the performance of ceramic pellets is
221 dominant. It can be seen from Fig. 7(i) that pores are wrapped in grains, indicating that the grain
222 boundaries move rapidly with 7 wt% Bi₂O₃ at 620°C, which leads to a decline in its mechanical
223 properties. In addition, it can be seen from Fig. 2 that the density of Bi₂O₃–PbO ceramic pellets drops
224 sharply when the Bi₂O₃ content exceeds 3 wt%, with almost the same grain size.

225 Figure 8 presents the SEM micrographs and fracture images of 3 wt% Bi₂O₃–97 wt% PbO sintered
226 at 570°C and 670°C. Also, obvious powder agglomeration is observed in Fig. 8(a) and (b), indicating
227 that sintering is not complete at this low temperature (570°C). Thus, grain growth plays a leading
228 role in enhancing hardness and flexural strength at lower temperature (570°C). However, at 670°C,
229 microcracks are observed on the surface of 3 wt% Bi₂O₃–97 wt% PbO ceramic pellets (Fig. 8(c)). They
230 are apt to appear at the interface of two ceramic grains and readily propagate through the grains,
231 which causes their hardness and strength to be lower than those of the ceramic pellets at 620°C. Thus,
232 the optimum sintering temperature and doping amount of Bi₂O₃ for Bi₂O₃–PbO ceramic pellets are
233 determined to be 620°C and 3 wt%, respectively.

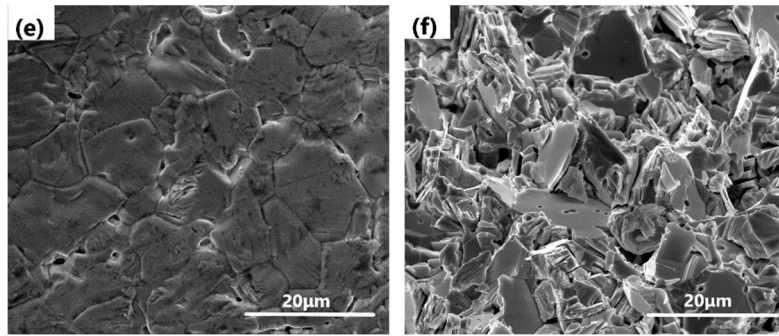
234

235

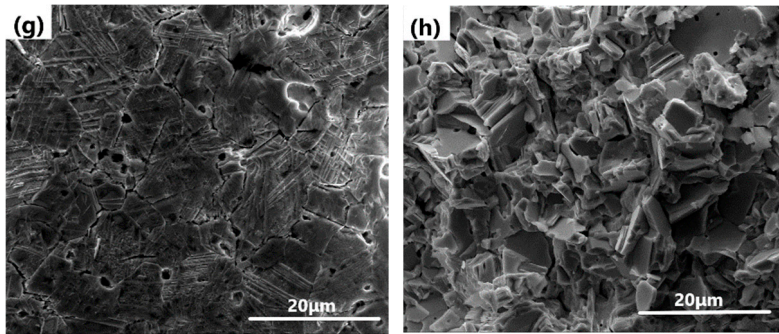
236



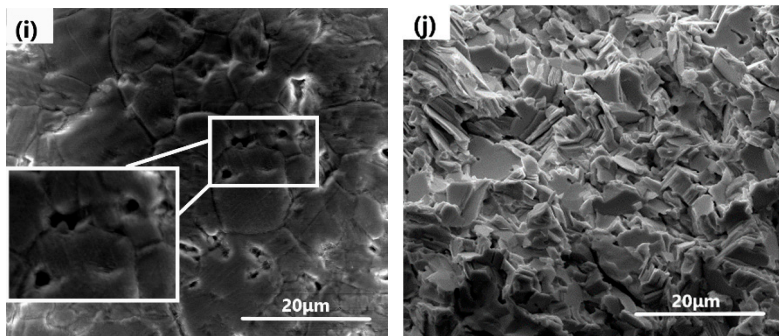
237



238



239



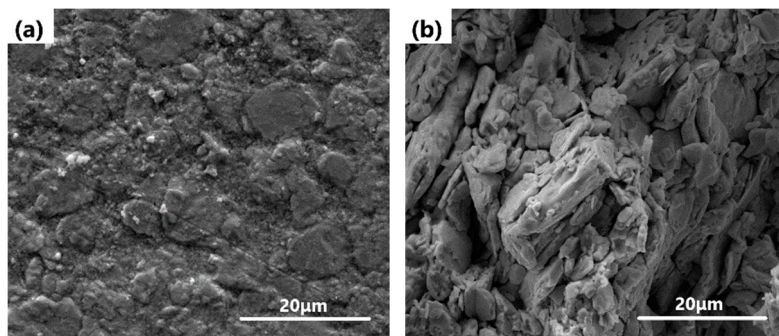
240

241

242

Figure 7. SEM micrograph and fracture images of PbO ceramic pellets sintered at 620°C with different Bi₂O₃ content (a, b) 0 wt%, (c, d) 1 wt%, (e, f) 3 wt%, (g, h) 5 wt%, (i, j) 7 wt%.

243



244

245

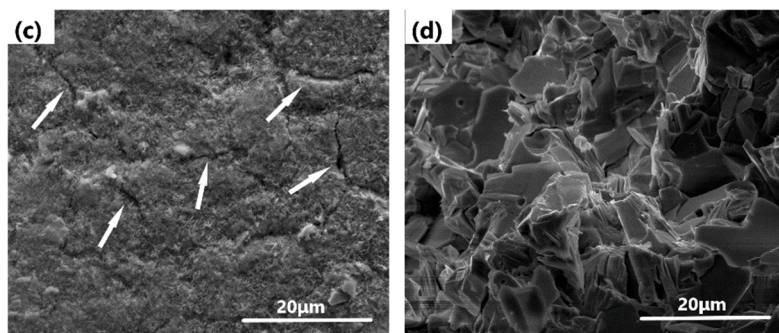


Figure 8. SEM micrographs and fracture images of 3 wt% Bi₂O₃–97 wt% PbO

246 sintered at (a, b) 570°C, and (c, d) 670°C.

247 5. Conclusions

248 In this paper, the effects of doping of Bi₂O₃ and sintering temperatures on the mechanical
249 properties of PbO ceramic pellets were investigated. It was found that doping with a moderate
250 amount of Bi₂O₃ could significantly enhance the mechanical properties of PbO ceramic pellets. The
251 enhancement is attributed to the formation of solid solution of Bi³⁺ ions. The optimal sintering
252 temperature and doping amount of Bi₂O₃ are 620°C and 3 wt%, respectively, for PbO. The hardness
253 increased four times and the strength increased two times as compared with pure PbO. The ceramic
254 pellets showed good performance in the LBE flushing experiment.

255 6. Patents

256 The method of bismuth oxide reinforced lead oxide ceramics introduced in this paper has been
257 applied to China Patent Office for an invention patent.

258

259 **Author Contributions:** Conceptualization, Yan Ma; Funding acquisition, Huiping Zhu; Investigation, Anxia
260 Yang; Methodology, Yan Ma and Anxia Yang; Project administration, Fenglei Niu; Writing – original draft, Yan
261 Ma and Anxia Yang; Writing – review & editing, Yan Ma, Anxia Yang, Huiping Zhu, Arslan Muhammad,
262 Pengwei Yang and Bokun Huang.

263 **Funding:** This research was funded by the National Natural Science Foundation of China (Grant No. 11705059,
264 11635005, 11705058), the Beijing Natural Science Foundation (Grant No. 2162040, 1192016) and the Fundamental
265 Research Funds for the Central Universities (Grant Nos.2018ZD10).

266 **Acknowledgments:** The support of Science and Technology on Reactor System Design Technology Laboratory
267 is also grateful.

268 **Conflicts of Interest:** The authors declare no conflict of interest.

269 References

- 270 1. B. F. Gromov; Yu. S. Belomitcev. Use of lead-bismuth coolant in nuclear reactors and accelerator-driven
271 systems. *Nucl. Eng. Des.* **1997**, *173*, 207-217. 10.1016/S0029-5493(97)00110-6.
- 272 2. J. Zhang; N. Li. Review of the studies on fundamental issues in LBE corrosion. *J. Nucl. Mater.* **2008**, *373*, 351-
273 377. 10.1016/j.jnucmat.2007.06.019.
- 274 3. OECD. Handbook on Lead–bismuth Eutectic Alloy and Lead Properties, Materials Compatibility, Thermal-
275 hydraulics and Technologies. <http://www.oecd-nea.org/science/reports/2007/nea6195-handbook.html>.
- 276 4. P. N. Martinov; R. S. Askhadullin; A. A. Simakov. Designing mass exchangers for control of oxygen content
277 in Pb-Bi (Pb) coolants in various research facilities. International Conference on Nuclear Engineering **2009**,
278 *1*, 555-561. 10.1115/ICONE17-75506.
- 279 5. Marino A.; Lim J. I. A mass transfer correlation for packed bed of lead oxide spheres in flowing lead
280 bismuth eutectic at high Péclet numbers. *Int. J. Heat Mass Tran.* **2015**, *80*, 737-747.
281 10.1016/j.ijheatmasstransfer.2014.09.079.
- 282 6. M. Kondo; M. Takahashi. Study on control of oxygen concentration in lead–bismuth flow using lead oxide
283 particles. *J. Nucl. Mater.* **2006**, *357*, 97-104. 10.1016/j.jnucmat.2006.05.051.
- 284 7. L. Brissonneau; F. Beauchamp. Oxygen control systems and impurity purification in LBE: Learning from
285 DEMETRA project. *J. Nucl. Mater.* **2011**, *415*, 348-360. 10.1016/j.jnucmat.2011.04.040.
- 286 8. S. Y. Zhang. Sintering and performance of lead oxide ceramics used for solid phase oxygen control system
287 in LBE (in Chinese). Dissertation for Master Degree. North China Electric Power University, Beijing, China,
288 2016.
- 289 9. Y. Ma; S. Y. Zhang. Sintering behavior of lead oxide ceramic prepared by microwave sintering. *Adv. Mater.*
290 *Res.* **2014**, *941-944*, 525-528. 10.4028/www.scientific.net/AMR.941-944.525.
- 291 10. M. Venkata Ramana; S. Roopas Kiran. Investigation and characterization of Pb(Zr_{0.52}Ti_{0.48})O₃
292 nanocrystalline ferroelectric ceramics: By conventional and microwave sintering methods. *Mater. Chem.*
293 *Phys.* **2011**, *126*, 295-300. 10.1016/j.matchemphys.2010.11.023.

- 294 11. A. I. Kingon; J. B. Clark. Sintering of PZT Ceramics: I, atmosphere control, II, effect of PbO content on
295 densification kinetics. *J. Amer. Cera. Soc.* **1983**, *66*, 253-256. 10.1111/j.1151-2916.1983.tb15709.x.
- 296 12. ASTM C1327-15, Standard Test Method for Vickers Indentation Hardness of Advanced Ceramics. ASTM
297 International, West Conshohocken, PA, 2015, www.astm.org.
- 298 13. O. Thomas; Z. Alexander. Evolution of young's modulus, strength, and microstructure during liquid-phase
299 sintering. *J. Amer. Cera. Soc.* **1998**, *81*, 195-200. 10.1111/j.1151-2916.1998.tb02557.x.
- 300 14. T. Y. Liu; Y. M. Li. Effect of Pr inoculation and crystal size on the Hall-Petch relationship for Al-
301 30 wt%Mg₂Si composites. *Mater. Lett.* **2018**, *214*, 6-9. 10.1016/j.matlet.2017.11.105.
- 302 15. S. G. Guo. Powder Sintering Theory (in Chinese), 1st ed. Metallurgical Industry Press: Beijing, China, 1998;
303 pp.292-295.
- 304 16. N. Liu; Y. D. Xu. Influence of molybdenum addition on the microstructure and mechanical properties of
305 TiC-based cermets with nano-TiN modification. *Ceram. Int.* **2003**, *29*, 919-925. 10.1016/S0272-
306 8842(03)00046-4.